Acta Technica Napocensis: Civil Engineering & Architecture Vol. 56, No. 2 (2013)
Journal homepage: http://constructii.utcluj.ro/ActaCivilEng
Special Issue: First International Conference for PhD Students in Civil Engineering, CE-PhD 2012.

Seismic assessment of an existing Hungarian highway bridge

József Simon[*1], László Gergely Vigh[2]

[1,2] *Budapest University of Technology and Economics, Department of Structural Engineering*
H-1521 Budapest, Műegyetem rkp. 3., Hungary

(Accepted 28 August 2013; Published online 30 September 2013)

Abstract

In this paper a case study of a typical Hungarian highway bridge is presented, illustrating the seismic performance and damage evaluation method. The investigated large-span bridge consists of continuous steel box-section superstructure supported by reinforced concrete piers. For the analysis, a sophisticated beam-element numerical model is developed. Linear spectral response analysis as well as non-linear static and cyclic analyses are invoked for the evaluation, then their results are compared. The model incorporates non-linear characteristics of the critical details, such as pier, pier-to-superstructure joints, etc. Pushover and incremental dynamic analysis using several earthquake records is applied to determine the fragility curves reflecting the probability of various damage occurrences. The analyses indicate that the most vulnerable component is the fixed bearing, the collapse of the whole structure is caused by the local failure of the restrained pier, and the structure provides relatively large extra resistance against seismic loads.

Keywords: Eurocode 8 analysis methods, time-history analysis, non-linear analysis, pushover analysis, seismic assessment of continuous girder bridge, incremental dynamic analysis, fragility curve

1. Introduction

In low or moderate seismicity regions, such as Hungary, bridges conventionally used to be designed with no or minimal consideration of seismic loads. In 2006 a new seismic hazard map was released with an increased seismic proneness, classifying Hungary as moderate seismic zone. According to experiences on newly erected structures in the last decade [1], [2] and parametric study on typical continuous girder bridges of Hungary [3], many of the girder bridges are vulnerable to earthquake loads calculated in accordance with Eurocode 8 [4], [5] even in moderate seismic regions. Specific components such as piers, foundations and bearings can suffer severe damage. Special care should be taken in case of the assessment of existing structures because of the possible lack of knowledge of material properties and stiffness values. In order to achieve sufficient seismic performance, critical details and elements may have to be reinforced even though they would be safe in ultimate limit state.

The global scope of our research is to evaluate the seismic performance and the expected damage during the lifetime of existing and newly erected Hungarian bridges on the basis of performance based design methodology [6]. Based on the results, possible retrofit methods for existing bridges as well as proper design concept for newly erected bridges may be proposed.

[*] Corresponding author. Tel./ Fax.: +36 30 425 26 25
E-mail address: j.simon.bme@gmail.com

In this paper which is a revised and extended version of a paper that was presented at CE-PhD 2012 [7], a typical continuous girder bridge, the M0 Háros highway bridge in Hungary is examined. A three dimensional numerical model incorporating non-linear characteristics of the critical details is developed in Open System for Earthquake Engineering Simulation FEM software (OpenSEES) [8]. According to EC 8-2 [5] conventional linear spectral response analysis is first carried out to compute probable reaction forces and displacements. Secondly, to determine the collapse mechanisms, non-linear static pushover analysis is applied. Finally, to capture the actual seismic behavior of the bridge and to characterize the possible reserve capacity, non-linear time-history analysis is completed. Based on the results, the critical structural components influencing the overall seismic performance are determined. To evaluate the feasibility of the different analysis methods, results are compared to each other on the level of internal forces in the critical elements. Finally, incremental dynamic analysis based stochastic assessment is used to create fragility curves of the critical components and to evaluate more precisely the actual seismic performance of the bridge.

2. Bridge description

The case study bridge is a newly erected highway bridge over the Danube River for the M0 Motorway at Háros. The total length of the bridge is *770.42m* (*3x73,5m* flood, *3x108,5m* river and *3x73,5m* flood bridges) and the total width of the deck is *21.80m* (*1.9m* sidewalk + *18.0m* carriageway + *1.9m* sidewalk). The river bridge is a continuous three span girder with a one-cell box cross-section with inclined webs and an orthotropic deck. The flood bridges are three span continuous composite bridges. The steel box is identical to that of the river bridge, but the deck is a R.C. slab. The bridge is straight in plan. In this study only the river bridge is analyzed. The river bridge shares two common piers with the flood bridges (pier 4 and pier 7) and is separated from the flood bridges by a *±70 mm* (pier 4) and a *±160 mm* (pier 7) expansion joint. In the longitudinal direction the girder of the river bridge is restrained only at pier 5. The longitudinal view of the bridge can be seen in Figure 1.

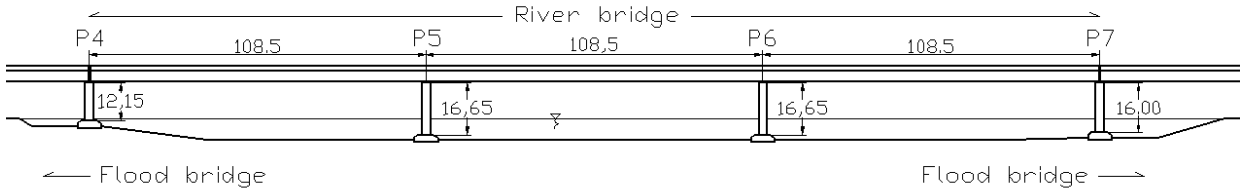

Figure 1. Longitudinal section of the river bridge.

Table 1. Cross-sectional data.

Girder	S1	S2	S3	S4
A [m²]	0.82	0.91	1.11	1.15
Iy [m⁴]	3.20	4.08	5.75	5.84
Iz [m⁴]	23.50	24.50	25.80	26.90
It [m⁴]	4.83	5.77	6.52	7.05
P4	S1	S2	S3	S4
A [m²]	23.7	27.4	36.4	108.0
Iy [m⁴]	14.1	11.9	23.4	393.0
Iz [m⁴]	486.0	432.0	518.0	2430.0
It [m⁴]	34.4	35.3	81.1	1170.0
P5	S1	S2	S3	S4
A [m²]	24.2	28.5	39.9	158.0
Iy [m⁴]	14.4	12.7	29.4	812.0
Iz [m⁴]	489.0	435.0	598.0	5350.0
It [m⁴]	35.7	39.4	101.0	2450.0
P6	S1	S2	S3	S4
A [m²]	24.2	28.5	39.9	158.0
Iy [m⁴]	14.4	12.7	29.4	812.0
Iz [m⁴]	489.0	435.0	598.0	5350.0
It [m⁴]	35.7	39.4	101.0	2450.0
P7	S1	S2	S3	S4
A [m²]	24.2	27.6	39.9	172.0
Iy [m⁴]	14.4	12.1	29.4	976.0
Iz [m⁴]	489.0	433.0	598.0	6230.0
It [m⁴]	35.7	36.1	101.0	2930.0

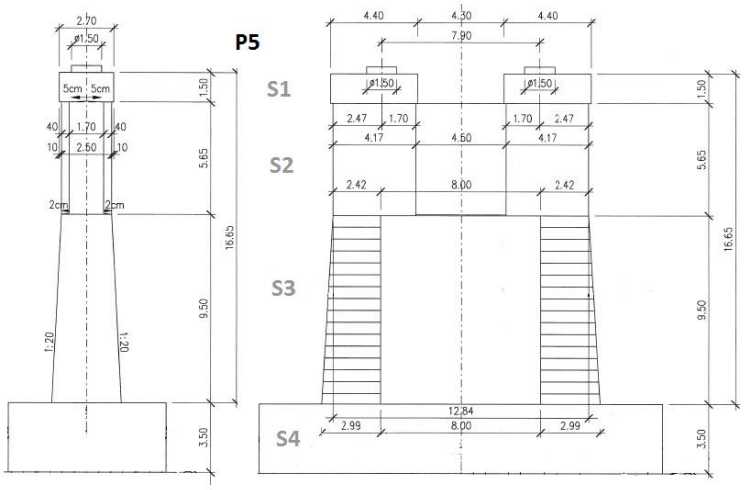

Figure 2. Side-views of pier 5.

The steel grade of the box girder is S355, the piers are made of C35/45 concrete and the reinforcing steel is grade S500B. The variable cross-section parameters of the box girder and the piers are listed in Table 1. The two side-views of pier 5 are shown in Figure 2. The cross-sections are nearly the same at each pier, only the pier height varies. The superstructure is fixed in the longitudinal direction at pier 5, whereas one of the two bearings provides lateral restraint at each pier.

In accordance with Eurocode 8 Part 2, the applied seismic parameters are as follows: ground acceleration of *0.1g*, soil type *C*, importance class *II*, type *1* spectrum. The applied mass is calculated from the dead loads and *1.0kN/m*^{2} live load distributed on the carriageway. This leads to an equivalent *146kN/m* distributed line load along the length of the girder.

3. Numerical model

3.1. Global properties of the numerical model

According to the comprehensive literature overview of [9] on seismic numerical modeling of girder bridges, a three dimensional numerical model is developed in OpenSEES [8]. A schematic picture of the numerical model can be seen in Figure 3.

The main structure, the girder and the piers are modeled by simple beam elements. The beam elements are placed in the center of gravity, and eccentricity between the member axis – such as axis of the superstructure and bearings placed on pier top – is bridged over by the help of rigid elements. The same rigid elements are used to model the eccentricity of the pier foot and pile cap. The bearings on the piers and the abutments are modeled by zero-length elements with linear or non-linear spring characteristics - depending on the analysis type - assigned to three degrees of freedom (u_x, u_y, u_z), but rotations are free to develop.

Each node has six degrees of freedom. Beam mesh size is typically one meter along the girder and the piers. This results in approximately *550* nodes (*~3300* DOFs) and approximately *540* elements applied in the final model, which is found sufficient to efficiently achieve results with an acceptable accuracy.

Since linear and non-linear analyses are also invoked in our investigation two different models are used which differ mainly in material models and material properties and are presented in the

following sub-sections.

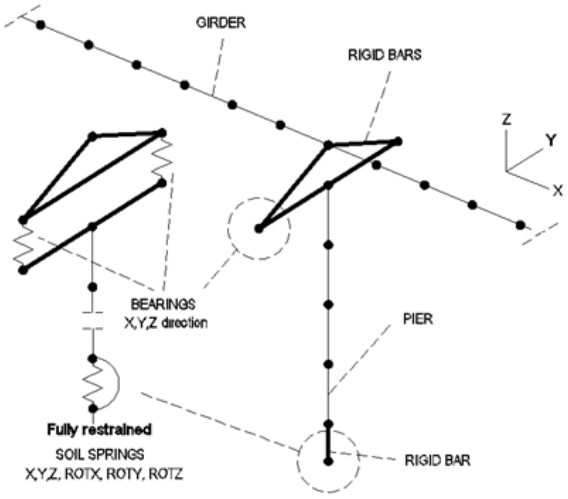

Figure 3. Numerical model of the bridge.

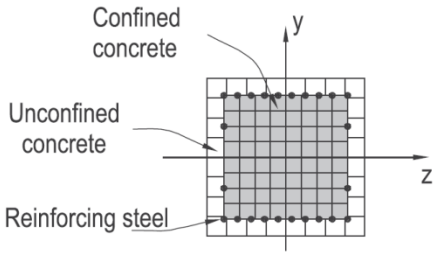

Figure 4. Fiber section [10].

3.2. Linear model

Linear model (LM) is used for the linear response spectrum analysis and the linear time-history analysis. In this case, geometric and material non-linearity is ignored. Accordingly, both the girder and the piers are modeled with elastic beam elements. The cross-sectional properties can be seen in Table 1. The elastic and shear moduli of the girder are: *E=210GPa*, *G=80.77GPa*; and of the concrete piers are: *E=32GPa*, *G=13.7GPa*.

According to Hungarian design conventions, it is assumed that fixed bearings are fully rigid, while expansion bearings provide no restraint in the model. (Note that, in the advanced analysis discussed in the following sections influence of the actual rigidity of the bearings is investigated.) A linear spring stiffness of *1e10N/m* is adjusted to the fully rigid connections.

The soil-structure interaction at the foundations of the piers is taken into account with integrate linear springs, adjusted with stiffness values (Table 3) calculated from foundation analysis.

Table 2. Bearing properties.

Type	Fixed	Expansion
K_1 [kN/mm]	70.0	14.0
K_1 [kN/mm]	10.5	0.1
F_y [kN]	960	5

Table 3. Foundation stiffness.

Pier No.	4	5	6	7
K_x [MN/m]	4760	3850	3850	3070
K_y [MN/m]	5130	4550	4550	3220
$K_{\phi x}$ [MNm/rad]	350000	500000	500000	350000
$K_{\phi x}$ [MNm/rad]	111000	125000	125000	111000

3.3. Non-linear model

Non-linear model (NLM) is used in case of push-over and non-linear time-history analyses as well as for incremental dynamic analysis. As the girder is expected to remain elastic during a seismic event, it is modeled with elastic beam element. However, due to the expected plastic deformations,

displacement based fiber section element is used (see Figure 4) for the piers.

The fibers have their own uniaxial stress–strain relationship. This way the cross-section is discretely modeled, and the confined and unconfined concrete regions as well as the longitudinal steel reinforcement can be taken into account. Since existing bridges are normally not designed for seismic events, sufficient confinement cannot be assumed. Conservatively, only unconfined concrete properties are applied in the numerical model of the M0 Háros bridge. For the behavior of reinforcing steel the Giuffré-Menegotto-Pinto model [11] (Steel02 material in OpenSEES, see Figure 5), and for the behavior of concrete linear tension softening concrete material model [12] (Concrete02 material model in OpenSEES, see Figure 6) is adopted. According to EC8, if non-linear analysis is carried out material properties should be taken into account with mean values. These values are calculated by assuming lognormal distribution and are presented in Table 4.

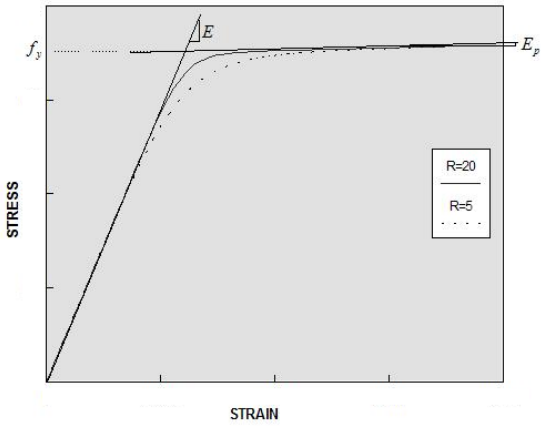

Figure 5. Giuffré-Menegotto-Pinto steel model [10].

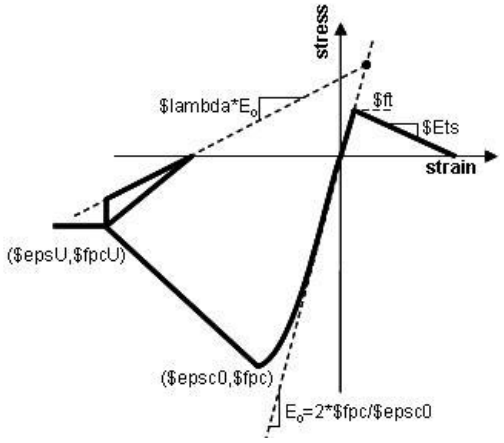

Figure 6. Linear tension softening concrete model [10].

For the elastomeric bearings bi-linear hysteretic material model is used (Figure 7). This behavior can be described by the initial stiffness (K_1), the post-yield stiffness (K_2) and the yielding strength (F_y). Table 2 shows the properties of the fixed and expansion bearings.

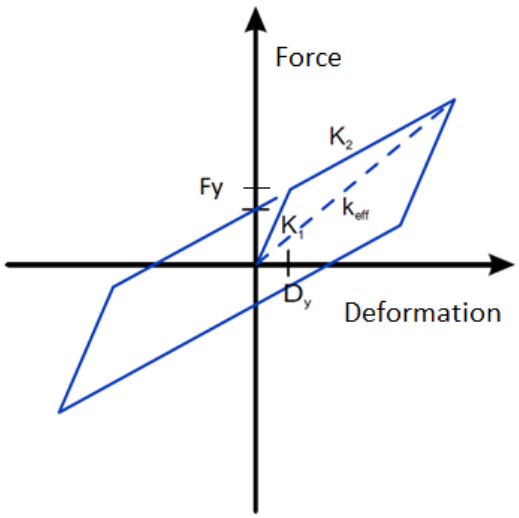

Figure 7. Bi-linear model of the bearings.

Unconfined concrete (C35/45)		
f_{pc} [MPa]	43	concrete compressive strength at 28 days
e_{psc0} [%]	0.225	concrete strain at maximum strength
f_{pcu} [MPa]	8.6	concrete crushing strength
e_{psu} [%]	0.350	concrete strain at crushing strength
λ [-]	0.1	ratio between unloading slope and initial slope
f_t [MPa]	3.2	tensile strength
E_{ts} [MPa]	32	tension softening stiffness
Reinforcing steel (S500B)		
F_y [MPa]	572	yield strength
E_0 [GPa]	224	initial elastic tangent stiffness
b [-]	0.01	strain-hardening ratio
R0 [-]	18	parameters to control the transition from elastic to plastic branches
CR1 [-]	0.925	
CR2 [-]	0.15	
a1,a2,a3,a4 [-]	-	hardening parameters (not used)

Table 4. Material properties for the NLM (mean values).

Three damage states are defined in the NLM to evaluate the seismic performance of the structure (see Section 5). The damage is measured in deformation and in curvature ductility ($\mu=\varphi_u/\varphi_y$) in case of the fixed bearing and the piers, respectively. The corresponding values are *50mm*, *100mm*, *150mm* of deformation and μ = *1, 4* and *7* curvature ductility for slight, moderate and full damages. These values are based on recommendations provided by HAZUS [13].

4. Comparison of analysis methods

The described linear (LM) and non-linear (NLM) models are applied for different analysis methods and compared to each other. The major results are discussed in the following sections.

4.1. Linear response spectrum analysis (LRSA)

Linear response spectrum analysis is the most commonly used earthquake analysis method among designers due to its relative simplicity and effectiveness. Original seismic design of the investigated structure was also made by LRSA. In the linear analysis, geometric and material non-linearity is ignored. Here the spring stiffness of the fixed bearings is set to model fully rigid connection. The effect of this modeling approximation is later investigated.

The linear dynamic analysis is carried out in accordance to EC8-2 [5]. The behavior factor (q) is *1.5* for the continuous girder (superstructure) as well as for the pier walls, and *q = 1.0* shall be used for the analysis and design of the bearings, abutments and foundations. The parameters of the standard acceleration response spectrum curve are: a_g = *1.0m/s*^{2}, soil type *C, M > 5.5,* ξ = *0.05*. The applied spectrums can be seen in Figure 8. Typical modal shapes and frequencies, obtained from the modal analysis, are illustrated in Figure 9. For typical continuous girder bridges with relatively flexible piers the first fundamental mode shape normally represents longitudinal motions [3]. In our case the piers stand in the Danube River, accordingly the cross-sections are robust, so the vertical stiffness of the girder is less than the longitudinal stiffness of the structure.

The internal and reaction forces are calculated by the CQC method. Results for the bearings and for the piers are summarized in Table 5. According to the analysis, the critical structural components are the longitudinally restrained pier 5 and its fixed bearings. The results show good accordance with [3].

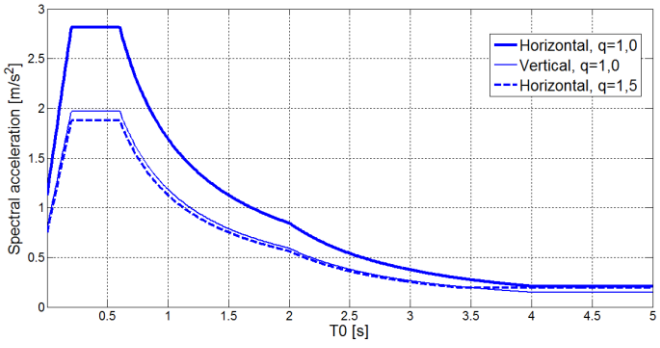

Figure 8. Applied standard response spectra.

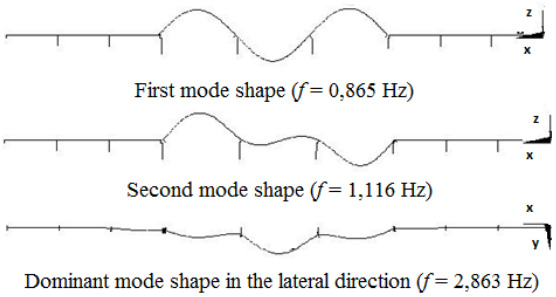

Figure 9. Typical modal shapes.

Here, only the representative results of the critical components are presented. The longitudinal (M_y) and transversal (M_x) moments of the longitudinally restrained pier are *229907kNm* and *275367kNm*, while the longitudinal (F_x) and transversal (F_y) reaction forces of the fixed bearing are *5075kN* and *7809kN*. The maximum displacements are *27mm* and *36mm* in the transversal (*y*) and longitudinal (*x*) directions, respectively; while the maximum deflection (mostly from the dead loads; in *z* direction) is *247mm*.

4.2. Linear time-history analysis (LTHA)

With time-history analysis the seismic behavior can be revealed more precisely since the structure is analyzed in the time domain in contrast to LRSA which generally overestimates the reaction forces in a conservative manner.

A new algorithm is developed in MATLAB [14] to create artificial acceleration records for time-history analysis. The records are determined to follow the given standard spectral acceleration curve (see Section 4.1. and Figure 8) within a defined range. According to EC 8-2, the 5%-damped elastic response spectrum of the design seismic action shall be used for the fitting and the defined period range is between *0,2T1* and *1,5T1*, where *T1* is the natural period of the fundamental mode of the structure. The difference between the original spectrum curve and the responses of the artificial record should be less than *10%*.

In preliminary study, the authors investigated the applicability of different artificial seismic record creation algorithms satisfying the EC criteria and found that the restriction of the fitting range is not sufficient if several modes are relevant, e.g. in the lateral direction. To bridge over this problem, the authors developed a new algorithm providing good matching in any period ranges.

The main idea of the algorithm is presented here. Common methods are based on minimizing the differences between the artificial motion's response spectrum and target spectrum in a least-square sense. Despite, the basic idea of the algorithm developed by the authors is to define the $\boldsymbol{A}$ amplitude vector (see Eq. 1) through iteration procedure. The function of the ground acceleration is assumed to be the sum of independent cosine waves with different frequency, amplitude and period shift. Therefore the following form is obtained:

$$a(t) = I(t) * \sum_{i=1}^{n} A_i \cos(\omega_i t + \varphi_i), \tag{1}$$

where A_i is the amplitude of the *i-th* cosine wave (initially *1.0* for each member), ω_i is calculated from the *i-th* natural period defined in advance:

$$\omega_i = \frac{2\pi}{T_i}, \tag{2}$$

φ_i is the *i-th* period shift randomly defined, and *I(t)* is the intensity function describing the intensity change of the ground motion during the seismic event. Figure 10 illustrates the proposed intensity function types. In our study, the linear function is used. The constant plateau should last for at least ten seconds if no seismic data is available for the construction site, thus the following time parameters are applied in accordance with Figure 10a: $t_1=4s$ (linear increase of intensity), $t_2=14s$ (end of the constant plateau; $t_2-t_1=10s$), $t_3=18s$ (end of the linear decrease and of the record).

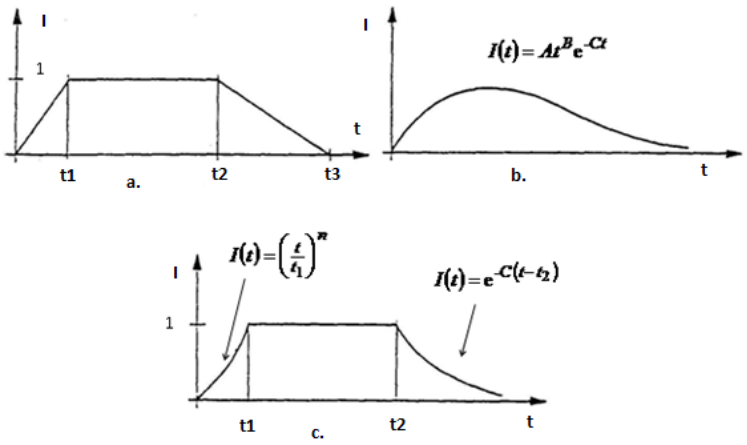

Figure 10. Intensity functions.

Once the *a(t)* function is created the acceleration response (SM_i^k) with different natural periods (*i* index) in the *k-th* iteration can be calculated by Newmark-β method. The values are compared to the standard values (SEC_i) and a correction vector is determined in each iteration:

$$r_i = \left[\frac{SEC_i}{SM_i}\right]. \tag{3}$$

At the end of the *k-th* iteration, the $\boldsymbol{A}$ vector should be multiplied by this correction vector:

$$\boldsymbol{A_{k+1}} = \boldsymbol{A_k} * \boldsymbol{r^T}. \tag{4}$$

The iteration is continued until each element of the $\boldsymbol{r}$ vector is close to *1.0* with a predefined tolerance. At the end of the iteration, adjustments have to be made to the *a(t)* artificial record to ensure that residual velocity and displacement are zero. For further information about the correction see [15].

As per EC8-2, at least three ground motion records (measured, synthetic or artificial) shall be used. In this case, the maximum values among the results belonging to the different seismic records shall be considered in the design (Figure 11); the corresponding extreme values are listed in Table 5.

It is confirmed that the LRSA is more conservative than the LTHA as the latter gives lower response values especially in the lateral direction. The longitudinal (M_y) and transversal (M_x) moments of the longitudinally restrained pier are decreased to *217218kNm* and *190599kNm*, while the longitudinal (F_x) and transversal (F_y) reaction forces of the fixed bearing are also lower: *4917kN* and *5202kN*. Despite, in both methods, piers and fixed bearings are found as critical elements. It is also observed that the maximum displacements are less than in case of LRSA: *34 mm*, *10mm* and *220mm* in the longitudinal, transversal and vertical directions, respectively.

4.3. Pushover analysis

As per EC8-2, pushover analysis (static non-linear analysis) can be applied for design check as alternative method to LSRA, or for characterizing the failure mechanisms. The load pattern applied in pushover analysis is basically determined by the most dominant mode shape, therefore if more modes are relevant (e.g. in the lateral direction) the method can be used only with limitations or multi-modal push-over analysis is needed. Generally in case of continuous girders with piers of moderate height (less than ~*25m*) one mode characterizes the seismic behavior in the longitudinal

direction [3], so pushover analysis could be a useful tool for capacity design, while results in the lateral direction are questionable. Accordingly, pushover analysis of the M0 Háros bridge is carried out only in this direction.

Table 5. Pier and bearing reaction forces from LRSA, LTHA and NLTHA (x - longitudinal; y - transversal; z - vertical directions).

Pier	Linear response spectrum analysis results					
	Fx	Fy	Fz	Mx	My	Mz
	kN			kNm		
4	2559	4211	32266	56145	20788	1004
5	13414	18430	89421	275367	229907	13838
6	11631	17175	89338	251826	88429	11
7	12599	16290	87876	175951	101845	5152

Pier	Linear response spectrum analysis results					
	Right bearing			Left bearing		
	Fx	Fy	Fz	Fx	Fy	Fz
	kN			kN		
4	0	1664	4422	0	0	4411
5	5045	7809	13198	5075	0	13186
6	0	7206	13037	0	0	13028
7	0	2003	4514	0	0	4508

Pier	Linear time-history analysis results					
	Fx	Fy	Fz	Mx	My	Mz
	kN			kNm		
4	2363	4027	31833	47126	17729	876
5	12188	11865	84309	190599	217218	11394
6	11403	11632	84138	174808	80323	9
7	11406	14846	82226	141237	98054	4218

Pier	Linear time-history analysis results					
	Right bearing			Left bearing		
	Fx	Fy	Fz	Fx	Fy	Fz
	kN			kN		
4	0	1241	3796	0	0	3898
5	4911	5202	12136	4917	0	12221
6	0	4702	11874	0	0	11956
7	0	1656	4057	0	0	4025

Pier	Non-linear time-history analysis results					
	Fx	Fy	Fz	Mx	My	Mz
	kN			kNm		
4	2344	5637	31871	63458	17146	1262
5	11744	10142	84419	159012	117741	12587
6	11219	11065	84360	160512	95641	101
7	10378	14046	82327	149178	113280	2461

Pier	Non-linear time-history analysis results					
	Right bearing			Left bearing		
	Fx	Fy	Fz	Fx	Fy	Fz
	kN			kN		
4	33	1027	3645	33	11	3589
5	1600	1330	10397	1600	18	10491
6	28	1371	10374	28	19	10455
7	26	1026	3691	26	11	3709

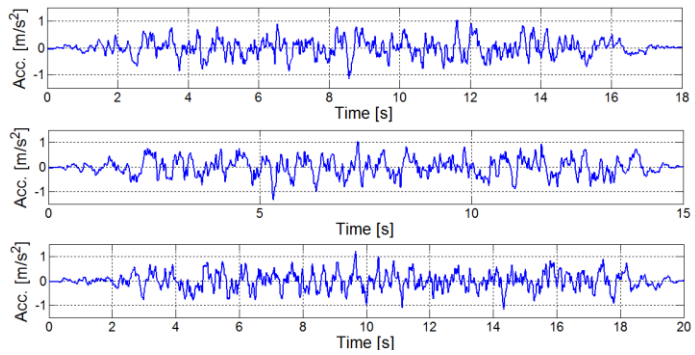

(a)

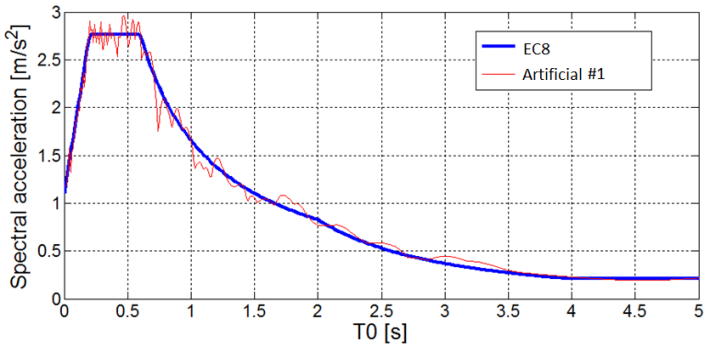

(b)

Figure 11. a- The fitted three artificial acceleration records; b- Responses from the first artificial record compared to the standard acceleration spectrum curve.

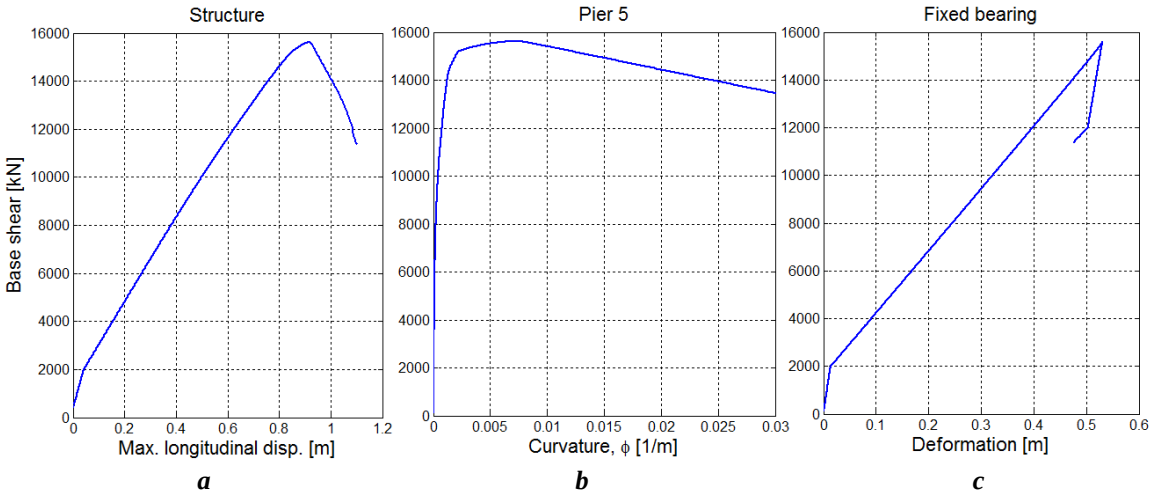

Figure 12. Capacity curves: a- for the whole structure; b- for the longitudinally restrained pier 5; c- for the fixed bearing.

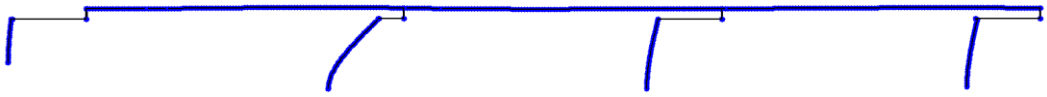

Figure 13. Collapse mechanism of the bridge in the longitudinal direction.

Capacity curves of the whole structure (base shear force vs. top displacement), the longitudinally restrained pier 5 (base shear force vs. curvature at the foot of the pier) and the fixed bearing (base shear force vs. deformation) are shown in Figure 12. The failure mechanism is illustrated in Figure 13. The analysis indicates that the ultimate collapse of the whole structure is caused by the local failure of the longitudinally restrained pier. However, failure/fracture is taken into consideration only in case of the piers in the simulations by using fiber sections. Considering *50mm*, *100mm* and *150mm* deformations as slight, moderate and full damage states proposed by HAZUS [13] for the fixed bearing, it can be realized that the fixed bearing suffers large deformations and bearing failure anticipates pier failure (corresponding pier curvatures are still in the linear region). Accordingly, the most vulnerable component is the fixed bearing. This indicates that the piers are robust, stiff, and provide relatively large extra resistance against seismic loads.

4.4. Non-linear time history analysis (NLTHA)

Non-linear dynamic analysis is the most rigorous analysis type. Note that the actual spring stiffness for representing the bearings results in increased fundamental period in the longitudinal direction (compare *0.725s* to *1.44s*), and a drastic drop in the seismic demand is expected on the basis of the response spectrum curve (Figure 8). Figure 14 compares the longitudinal bending moment and top displacement of Pier 5. The change in the natural period as well as the amplitude of the measured values is clearly observable.

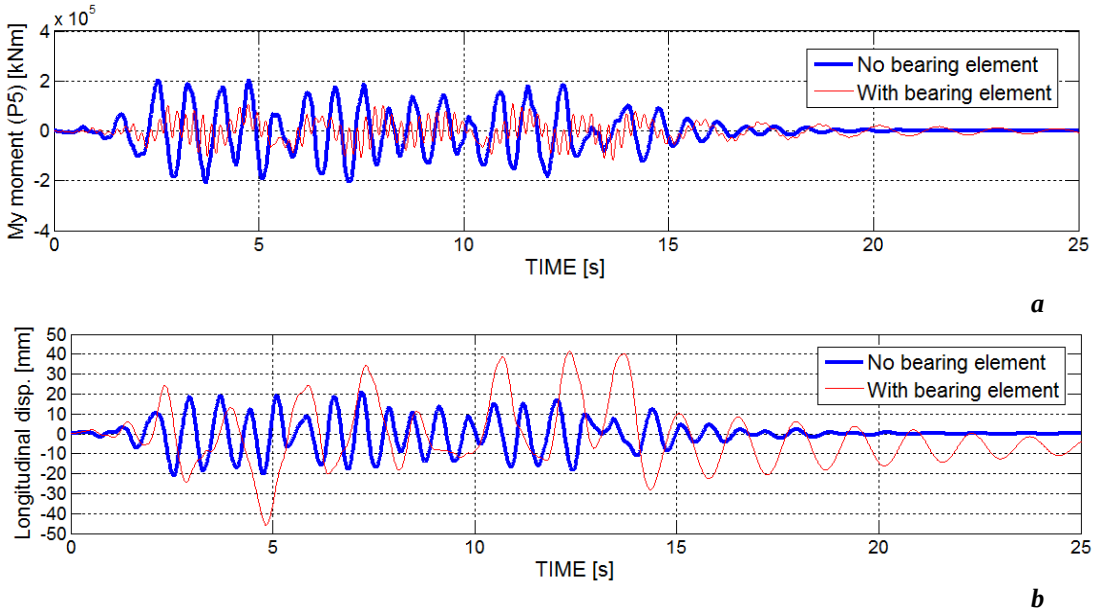

Figure 14. a- Longitudinal moment of pier 5 and b- longitudinal displacement of the structure with or without non-linear bearing elements.

The hysteretic behavior of the fixed and expansion bearings and of the longitudinally restrained pier computed from the first artificial record can be seen in Figure 15. In case of the piers the intensity of the record is upscaled by a factor of *1.25* to demonstrate the hysteretic behavior due to a stronger ground motion. The maximum moment calculated from the actual design intensity level is marked with thick horizontal lines. The hysteretic behavior of the pier indicates that the behavior is determined fundamentally by the behavior of the concrete, the energy dissipation of the pier is not sufficient.

The maximum deformations of the bearings are *42mm* and *67mm* in case of the fixed and expansion bearings, respectively. The deformation of the fixed bearing is less than the assumed slight damage level (*50mm*), thus no severe damage is expected.

Table 5 summarizes the bearing reaction forces and pier internal forces. The yielding of the fixed bearing decreases the maximum reaction force of the bearing, thus mitigates the lateral forces transferred to the longitudinally fixed pier and also the moments of the same pier. The longitudinal (M_y) and transversal (M_x) moments of the longitudinally restrained pier are now *117741kNm* and *159012kNm*, while the longitudinal (F_x) and transversal (F_y) reaction forces of the fixed bearing are also lower: *1600kN* and *1330kN*. Displacements of the girder in the longitudinal, lateral and vertical directions are *56mm*, *50mm* and *212mm.*

The calculated response (e.g. the plastic deformation, the displacements and also the internal forces) can be very sensitive to the characteristics of the individual ground motion used as seismic input, therefore a set of records should be used for higher reliability.

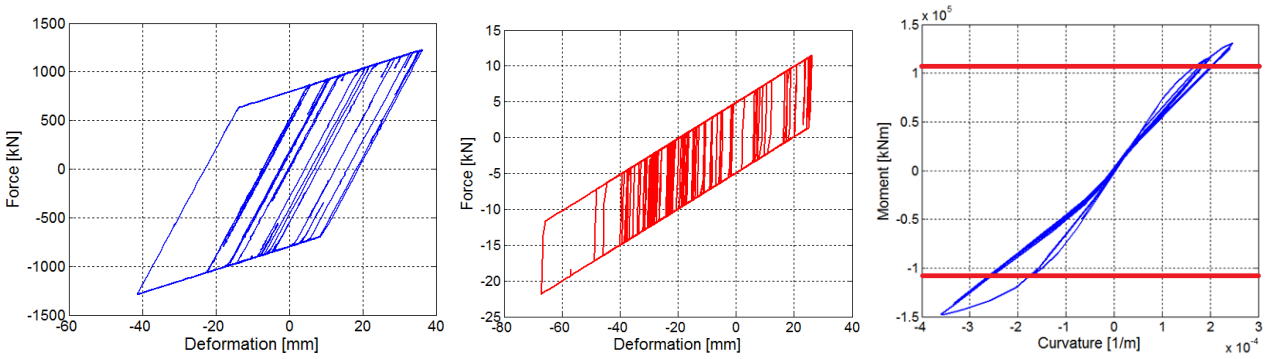

a ***b*** ***c***

Figure 15. Hysteretic behavior of the a- fixed and the b- expansion bearings and c- pier 5.

4.5. Comparison of the results

Reaction and internal forces from LRSA, LTHA and NLTHA are presented in Table 5. The representative results of the critical elements (the longitudinally restrained pier and the fixed bearing) and also the maximum longitudinal and transversal displacements of the girder is summarized in Table 6.

Analysis method	Pier moments		Bearing forces		Girder disp.	
	M_x [kNm]	M_y [kNm]	F_y [kN]	F_x [kN]	u_y [mm]	u_x [mm]
LRSA	275367	229907	7809	5045	27	36
THA	190599	217218	5202	4911	10	34
NLTHA	159012	117741	1330	1600	56	50

Table 6. Summary of the representative results from LRSA, THA and NLTHA.

It is found that LRSA is conservative in comparison to LTHA as the latter gives lower response values especially in the lateral direction. Since in the longitudinal direction one mode characterizes the seismic behavior, so it can be considered as an SDOF system, the two analyses lead to nearly the same results. The difference between the longitudinal moments (M_y) is only *5%*, while when the transversal moments (M_x) are observed, more than *40%* of difference is obtained. In both methods, the longitudinally fixed pier and the fixed bearing are found as critical elements.

The non-linear analysis methods also confirm that the most vulnerable component is the fixed bearing, whereas the piers are robust and stiff. The failure of the bearing anticipates the failure of the restrained pier, while the pier remains elastic at the level of bearing failure. The hysteretic behavior of the pier confirms that the pier is designed with minimal consideration of seismic loads, the energy dissipation of the pier during cyclic loading is not sufficient. For the given intensity level prescribed by the standard acceleration spectrum the bearing deformations are so low in the longitudinal direction that not even slight damage of the bearings and hereby of the piers are likely to occur.

The spring elements applied for the non-linear analysis decrease the stiffness of the structure and thus increase the fundamental period. The seismic responses are decreased, with increasing deformation demands. The responses obtained from NLTHA thus fundamentally differ from those of the linear analyses. While the longitudinal pier moments are decreased by 19%, the longitudinal displacements are increased by 32% compared to the LTHA. It can be also observed that the horizontal force transmission capability of the expansion bearings results more favorable reaction force distribution: the moments are lower at the restrained pier (pier 5) but higher at the non-restrained (pier 4, 6, 7) piers.

5. Incremental dynamic analysis (IDA)

The analysis methods discussed in the previous sections can highlight the most vulnerable components and details of the structure and they provide results for a given intensity level, but do not characterize the probability of failure of the structure. This probability can be expressed by creating the fragility curves of different components or the whole structure. The seismic performance can be very sensitive to the characteristics of the individual acceleration record. Following the instructions of FEMA P695 [16] document, incremental dynamic analysis is invoked using a set of *44* different ground motions. The earthquake records are sampled to provide a very diverse accelerogram set. First, this set is normalized by the peak ground velocities so that the variance of each record is reduced to an acceptable level. The normalized set then is scaled the way that the median acceleration response spectrum of the set equals the response spectrum used for the design at the fundamental period of the structure. The procedure is illustrated in Figure 16, where the scaling is completed at a period of *1.44s*, which corresponds to the dominant natural period of the non-linear model in the longitudinal direction. The analysis is carried out only in the critical longitudinal direction.

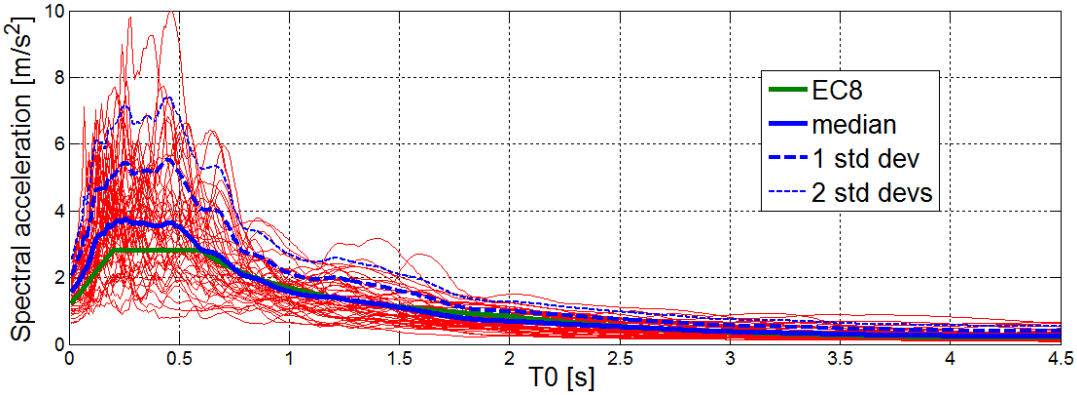

Figure 16. Response of the set of ground motion records scaled to a pre-defined spectral acceleration level at *T=1.44s*.

At each scaling level the maximum longitudinal displacement of the girder, the maximum curvature of the bottom section of the fixed pier and the fixed bearing deformation is registered for each ground motion. The displacement vs. spectral intensity – defined as the spectral acceleration – relation for each record is shown in Figure 17. Plateau of the curve corresponding to a seismic record (meaning rapidly increased deformations) indicates the structural collapse for the given record. Three damage levels (slight, moderate and full) are determined for each structural component. The damage is measured in deformation and in curvature ductility ($\mu=\varphi_u/\varphi_y$) in case of the fixed bearing and the piers, respectively. The corresponding values are *50mm*, *100mm*, *150mm* of deformation and μ = *1, 4* and *7* curvature ductility for slight, moderate and full damages. These values are based on recommendations provided by HAZUS [13]. According to this, fragility curves are created and shown in Figure 18.

The curves confirm the previous observation as the most vulnerable component in collapse prevention performance objective is the fixed bearing: the failure of the whole structure is determined by the full damage of the bearing (Figure 18 thick, solid line). Piers are so robust that they do not even suffer slight damage when the bearing is failed.

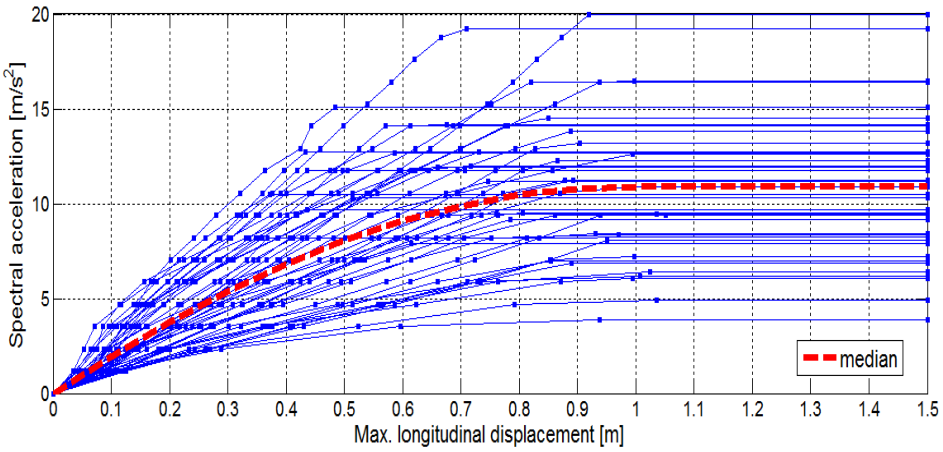

Figure 17. Maximum longitudinal displacement values from each ground motion record at different spectral acceleration levels.

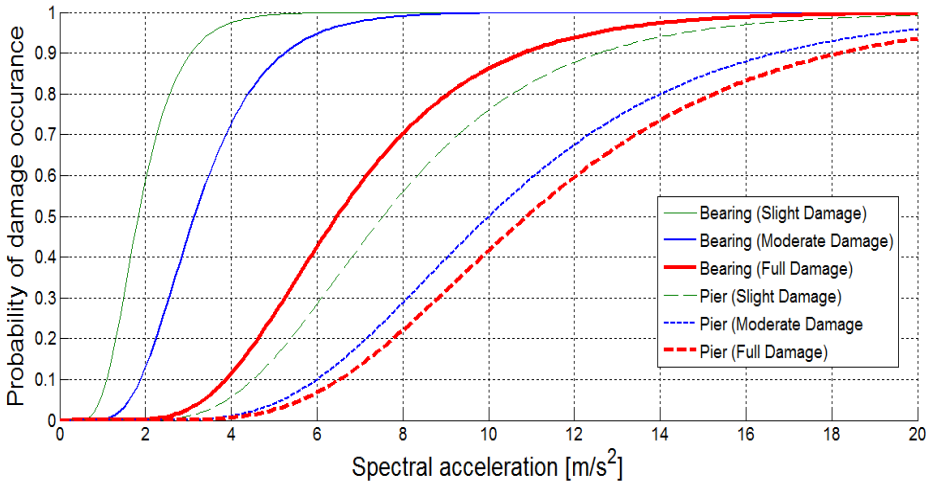

Figure 18. Fragility curves (slight, moderate and full damage) for the fixed bearing and the longitudinally restrained pier.

The standard spectral acceleration at the fundamental period (*1.44s*) is *1.175m/s*^{2}. The curves indicate that the actual seismic performance of the structure is sufficient: relatively large extra resistance against seismic loads is provided by the preserve material and cross-section capacities, even though the structure was not designed to ductile behavior.

The authors emphasize that the analysis is completed only to the longitudinal motions. Performance of the pier can be sensitive to the accompanying lateral effects and thus three-dimensional seismic analysis is necessary to investigate the actual failure probability.

6. Concluding remarks

In this paper the M0 Háros highway bridge in Hungary is investigated. Linear and non-linear analyses are carried out and compared to each other. The results confirm that the most vulnerable component is the fixed bearing, anticipating the failure of the restrained pier. Comparison of the analysis results shows that the LRSA overestimates the reaction forces and displacements compared to the LTHA, NLTHA methods. Using more sophisticated model incorporating non-linear elements results in more flexible structure, with decreased reaction forces and increased deformations.

In addition, incremental dynamic analysis based seismic performance assessment is completed in accordance to FEMA P695 [16]. The fragility curves created by incremental dynamic analysis indicate that the structure provides relatively large extra resistance against seismic loads due to the increased flexibility, and to the material and cross-section preserve capacity, even though the structure was not designed to ductile behavior.

7. References

[1] Joó A, Vigh LG, Kollár L. Experiences on seismic design of structures in Hungary. MAGÉSZ ACÉLSZERKEZETEK, Vol. 6:(1), pp. 72-81, 2009 (in Hungarian)

[2] Vigh LG, Dunai L, Kollár L. Numerical and design considerations of earthquake resistant design of two Danube bridges. Proc. ECEES 2006. Geneva, p. 10. Paper 1420, 2006

[3] Zsarnóczay Á. Seismic performance analysis of common bridge types in Hungary. Master Thesis at Budapest University of Technology and Economics, 2010 (in Hungarian)

[4] CEN: EN 1998-1:2008 Eurocode 8: Design of structures for earthquake resistance - Part 1: General rules, seismic actions and rules for buildings, 2008

[5] CEN: EN 1998-2:2008 Eurocode 8: Design of structures for earthquake resistance - Part 2: Bridges, 2008

[6] Deierlein GG. Overview of a Comprehensive Framework for Earthquake Performance Assessment. Performance-Based Seismic Design Concepts and Implementation. Proc. of Intl Workshop, PEER Report 2004/05, UC Berkeley, p. 15-26, 2004

[7] Simon J, Vigh LG. Seismic assessment of Hungarian highway bridges – A case study, Proc. First. Intl. Conf. PhD Students in Civil Engineering, pp. 155-162, Cluj-Napoca, 2012

[8] McKenna F, Feneves GL. Open system for earthquake engineering simulation. Pacific earthquake engineering research center, version 2.3.2., 2012

[9] Simon J. Numerical model development for seismic assessment of continuous girder bridges. Proceedings of the Conference of Junior Researchers in Civil Engineering, pp. 216-224. Budapest, Hungary, 2012

[10] http://opensees.berkeley.edu/

[11] Filippou FC, Popov EP, Bertero VV. Effects of Bond Deterioration on Hysteretic Behavior of Reinforced Concrete Joints. Report EERC 83-19, Earthquake Engineering Research Center, University of California, Berkeley, 1983

[12] Yassin MHM. Nonlinear Analysis of Prestressed Concrete Structures under Monotonic and Cycling Loads. PhD dissertation, University of California, Berkeley, 1994

[13] HAZUS. Earthquake loss estimation methodology. Technical Manual, National Institute of Building for the Federal EmergencyManageme nt Agency, Washington (DC), 1997

[14] MATLAB 2010b, The MathWorks, Inc., Natick, Massachusetts, United States, 2010

[15] Rezaeian S, Der Kiureghian A. Stochastic Modeling and Simulation of Ground Motions for Performance-Based Earthquake Engineering, PEER Center, University of California, 2010

[16] ATC: FEMA P695. Quantification of Building Seismic Performance Factors, 2009